Pergamon

Int. J. Heat Mass Transfer. Vol. 37, No. 18, pp. 3021–3025, 1994

0017-9310/94 $7.00+0.00

TECHNICAL NOTES

Convection in a porous medium with inclined temperature gradient: additional results

D. A. NIELD

Department of Engineering Science, University of Auckland, Private Bag 92109, Auckland, New Zealand

(*Received* 3 *November* 1993 *and in final form* 2 *March* 1994)

1. INTRODUCTION

Motivated by the belief that it serves as a paradigm for convection induced by an inclined applied temperature gradient in general situations, the author [1–3] has studied the case of such convection in a shallow layer of a saturated porous medium. The horizontal component of the applied gradient induces a Hadley circulation which, in the central portion of the flow, is approximately independent of horizontal position and can be treated as a uniform flow. This flow becomes unstable when the vertical component of the applied gradient is sufficiently great.

Linear stability analysis was first applied to this problem by Weber [4]. His analysis is limited to the case of small horizontal applied gradient. This limitation was lifted by Nield [1], who employed a Galerkin approximation in solving the resulting differential equation system. The problem reduces to the task of finding zeroes of a certain determinant of order $2N$, where N is the order of the Galerkin approximation. Because of the difficulty of handling determinants of high order, the report of Nield [1] was based on calculations with $N = 2$. These indicated that the additional convection appears in the form of stationary longitudinal rolls, and that, as the horizontal Rayleigh number R_H increases, the critical vertical Rayleigh number R_V also increases and there is a series of transitions to higher-order modes, corresponding to multiple layers of rolls. It was realized that, as R_H increases, the accuracy of the second-order approximation rapidly decreases, and the approximate results provide just upper bounds on the critical vertical Rayleigh number.

The author has now developed a new method of determining the zeroes of the determinants, and is able to handle calculations with $N = 8$. The more accurate results are now reported. It has been found that, rather than increasing indefinitely as R_H increases, the critical value of R_V reaches a maximum and then decreases, passing through zero at a certain value of R_H. This means that the new results predict that Hadley flow in a porous medium becomes unstable, even in the absence of an applied vertical gradient, when the circulation is sufficiently intense. This is an interesting result, because Gill [5] proved that the corresponding flow in a vertical slab is stable to small disturbances. Gill suggested that this is related to the absence of an inertial term in the Darcy equation, in contrast to the Navier–Stokes equation. (The non-linear analysis of Straughan [6] predicts that the flow is stable provided that the initial disturbance is smaller than a certain threshold. Rees [7] showed that the claim by Georgiadis and Catton [8] that the flow was unstable for a finite value of the Prandtl–Darcy number, was based on erroneous analysis.) Until now the stability of Hadley flow in a shallow cavity has been an open question. In their paper, Daniels *et al.* [9] did not investigate the stability of the flow, but merely commented that "porous media appear less prone to shear instabilities" (than clear viscous fluids).

A feature of the present problem is the way in which the form of the favoured disturbed flow changes dramatically as R_H increases. The eigenfunctions (as well as eigenvalues) of the differential equation system are now calculated, and representative streamline patterns are presented.

BASIC EQUATIONS AND STEADY STATE SOLUTION

In order to improve the presentation, scaling different from that of Nield [1] (who followed Weber [4]) is now introduced, and some of the other notation is changed. Cartesian axes are chosen with the z^*-axis vertically upwards and the x^*-axis in the direction of the applied horizontal temperature gradient β_T. The superscript asterisks denote dimensional variables. The porous medium occupies a layer of height H. The vertical temperature difference across the boundaries is ΔT. It is assumed that the Oberbeck–Boussinesq approximation is valid, and that flow in the porous medium is governed by Darcy's law. Accordingly the governing equations are

$$\nabla^* \cdot \mathbf{v}^* = 0, \tag{1}$$

$$0 = -\nabla^* P^* - (\mu/K)\mathbf{v}^* + \rho_f^* \mathbf{g}, \tag{2}$$

$$(\rho c)_m(\partial T^*/\partial t^*) + (\rho c_P)_f \mathbf{v}^* \cdot \nabla^* T^* = k_m \nabla^{*2} T^*, \tag{3}$$

$$\rho_f^* = \rho_0[1 - \gamma_T(T^* - T_0)]. \tag{4}$$

Here $(u^*, v^*, w^*) = \mathbf{v}^*$, P^* and T^* are the seepage (Darcy) velocity, pressure and temperature, respectively. The subscripts m and f refer to the porous medium and the fluid respectively. Also μ, ρ and c denote viscosity, density and specific heat, while K is the permeability of the medium, k_m is the thermal conductivity and γ_T is the thermal expansion coefficient.

The boundary conditions are

$$w^* = 0, \quad T^* = T_0 - (\pm\Delta T)/2 - \beta_T x^*, \quad \text{at } z^* = \pm H/2. \tag{5}$$

We define non-dimensional quantities by $\mathbf{x} = \mathbf{x}^*/H$, $t = \alpha_m t^*/AH^2$, $(u, v, w) = \mathbf{v} = H\mathbf{v}^*/\alpha_m$, $P = K(P^* + \rho_0 g z^*)/\mu\alpha_m$, $T = R_V(T^* - T_0)/\Delta T$, where $\alpha_m = k_m/(\rho c_P)_f$, $A = (\rho c)_m/$

NOMENCLATURE

A	heat capacity ratio, $(\rho c)_m/(\rho c_P)_f$
A_{ij}	matrix element
c	specific heat
D	differential operator, d/dz
g	gravitational acceleration
H	layer height
$\mathbf{i}, \mathbf{j}, \mathbf{k}$	unit vectors
k	thermal conductivity
K	permeability
l, m	dimensionless wavenumbers in the x- and y-directions
N	order of Galerkin approximation
P	dimensionless pressure (excess over hydrostatic)
Pr	Prandtl number
R_H	horizontal Rayleigh number, $\rho_0 g \gamma_T K H^2 \beta_T/\mu\alpha_m$
R_V	vertical Rayleigh number, $\rho_0 g \gamma_T K H \Delta T/\mu\alpha_m$
t	dimensionless time
$\tilde{T}(z)$	dimensionless vertical variation of the basic temperature
ΔT	temperature difference between lower and upper boundaries
$U(z), V(z)$	dimensionless steady state velocity components
$\mathbf{v}$	dimensionless velocity vector
x, y, z	dimensionless Cartesian coordinates.

Greek symbols

α	dimensionless overall horizontal wavenumber
α_m	thermal diffusivity, $k_m/(\rho c_P)_f$
β_T	horizontal temperature gradient
γ_T	coefficient of volume expansion
θ	dimensionless temperature perturbation
κ	thermal diffusivity
μ	dynamic viscosity
ν	kinematic viscosity
ρ	density
σ	dimensionless frequency for disturbances.

Subscripts

c	critical
s	steady state
0	standard.

Superscripts

$'$	perturbation quantities
$*$	dimensional variables.

$(\rho c_P)_f$, $R_V = \rho_0 g \gamma_T K H \Delta T/\mu\alpha_m$. We refer to R_V as the vertical thermal Rayleigh number. We also introduce the horizontal Rayleigh number R_H defined by

$$R_H = \rho_0 g \gamma_T K H^2 \beta_T/\mu\alpha_m. \tag{6}$$

The governing equations now take the form

$$\nabla \cdot \mathbf{v} = 0, \tag{7}$$

$$0 = -\nabla P - \mathbf{v} + T\mathbf{k}, \tag{8}$$

$$\partial T/\partial t + \mathbf{v} \cdot \nabla T = \nabla^2 T. \tag{9}$$

The boundary conditions are now

$$w = 0, \quad T = -(\pm R_V)/2 - R_H x, \quad \text{at } z = \pm 1/2. \tag{10}$$

Equations (7)–(10) have a steady state solution of the form:

$$T_s = \tilde{T}(z) - R_H x, \quad u_s = U(z), \quad v_s = 0, \quad w_s = 0,$$

$$P_s = P(x, y, z).$$

This is a solution provided that

$$DU = R_H,$$

$$D^2 \tilde{T} = -U R_H.$$

Here D denotes the derivative operator, d/dz. It is assumed that there is no net flow so $\langle U \rangle = 0$. Here, the angular brackets denote an average with respect to the vertical coordinate. The steady state solution is thus the Hadley circulation:

$$U = R_H z, \tag{11}$$

$$\tilde{T} = -R_V z + \frac{1}{24} R_H^2 (z - 4z^3). \tag{12}$$

STABILITY ANALYSIS

We now perturb the steady state solution. We write $\mathbf{v} = \mathbf{v}_s + \mathbf{v}'$, $T = T_s + \theta'$, $P = P_s + p'$. The linearized perturbation equations are

$$\nabla \cdot \mathbf{v}' = 0, \tag{13}$$

$$\nabla p' + \mathbf{v}' - \theta' \mathbf{k} = 0, \tag{14}$$

$$\partial\theta'/\partial t + U \partial\theta'/\partial x - R_H u' + (D\tilde{T}) w' = \nabla^2 \theta'. \tag{15}$$

We make the normal mode expansion

$$[u', v', w', \theta', p'] = [u(z), v(z), w(z), \theta(z), p(z)] \times \exp\{i(kx + ly - \sigma t)\}. \tag{16}$$

We substitute this into the perturbation equations and eliminate p, u and v from the resulting equations to obtain

$$(D^2 - \alpha^2) w + \alpha^2 \theta = 0, \tag{17}$$

$$(D^2 - \alpha^2 + i\sigma - ikU)\theta + i\alpha^{-2} k R_H D w - (D\tilde{T}) w = 0, \tag{18}$$

where $\alpha = (k^2 + l^2)^{1/2}$ is the overall horizontal wavenumber. We refer to a disturbance with $k = 0$ as a longitudinal mode and one with $l = 0$ as a transverse mode. The last two equations must be solved subject to appropriate boundary conditions. For the case of impermeable, isothermal boundaries, we have

$$w = \theta = 0 \quad \text{at } z = \pm\tfrac{1}{2}. \tag{19}$$

The problem is now reduced to that of solving equations (17)–(19), where

$$D\tilde{T} = -R_V + \frac{1}{24} R_H^2 (1 - 12z^2). \tag{20}$$

Without loss of generality, we may regard R_V as the eigenvalue, with R_H, σ, k and l as parameters. At neutral stability, σ has to be real and chosen so that R_V is real. Subject to this constraint, the critical value of R_V is its minimum as σ, k and l are varied.

NUMERICAL CALCULATIONS

Method

The standard Galerkin method yields an eigenvalue equation for R_V in terms of R_H, σ, k and l. One needs to calculate R_V as the smallest positive zero of the determinant of a certain determinant. For $N = 2$, it is feasible to expand the determinant (of order 4) in terms of its elements. For $N = 4$, it is feasible to evaluate the determinant using Gaussian elimination. For larger values of N the expansion involves an excessive number of terms and an alternative practical method is needed. One can force the determinant to zero by requiring the equivalent system of homogeneous equations to have a non-zero solution, and one can ensure this by imposing a suitable additional linear constraint. When the determinant is not zero no exact solution of the augmented system exists, but one can seek the solution which gives the best least-squares fit, and then locate a zero by minimizing the least-squares error. The author has written a FORTRAN program which employs the NAG subroutine F04JAF for this purpose. The subroutine also returns the eigenvector and from this the functions $w(z)$ and $\theta(z)$ can be determined.

Results

It was shown by Nield [1] that the favoured form of the disturbance is in the form of non-oscillatory longitudinal rolls, and accordingly the results reported in this paper are for $\sigma = 0$ and $k = 0$. For various values of R_H, R_V was calculated and minimized as a function of the horizontal wavenumber α. This gives the critical vertical Rayleigh number. The results presented in Table 1 are for $N = 8$ (corresponding to a complex-valued determinant of order 16 and an equivalent real-valued determinant of order 32). This was the largest value of N for which zeroes of the determinant could be successfully discriminated. The failure for larger N is presumed to be due to columns of the determinant losing their independence. This failure is of no consequence when R_H is small because the convergence as N increases is rapid. Comparisons with calculations with $N = 6$ indicate that the values of R obtained with $N = 8$ are in error by less than 1% when $R_H \leqslant 50$, but the accuracy deteriorates considerably for higher values of R_H. For $R_H = 100$ the error is about 10%. For larger values of R_H, the critical R_V is a rapidly changing function of R_H and it is easier to estimate the value of R_H for a given value of R_V rather than vice versa. For example, when $R_V = 0$ the value of the critical R_H with $N = 8$ is 132.5 and that with $N = 6$ is 138.3. The deterioration in accuracy of the Galerkin approximation of given order as R_H increases is presumably due to the eigenfunctions taking a form (with boundary layers and multiple peaks) which cannot be approximated closely by any low-degree polynomial.

A feature of the present problem is the way in which the form of the favoured disturbance changes as R_H increases. In Fig. 1 the eigenfunction $w(z)$, normalized so that its maximum magnitude is unity, is plotted for representative values of R_H. (In each case θ varies with z in much the same way as w does.) For $R_H = 0$ the profile is sinusoidal. As R_H increases to 70 the profile flattens in the middle and tends to develop a boundary layer near each horizontal boundary. For $R_H = 80$ the even mode is no longer the favoured one; it has been replaced by an odd one. [The calculations show that the coefficients of even terms in the Galerkin expansion are negligible in comparison with the odd ones at criticality. That the solutions have symmetry is expected because the differential equation system is invariant under the transformation $(y, z, k, l) \to (-y, -z, -k, -l)$.] It is noteworthy that the slope of the curve at intermediate values of z is almost constant. For $R_H = 132.5$ the favoured mode is again an even one, but the profile now has two peaks and a trough. The corresponding streamline patterns for the perturbation flow are presented in Fig. 2. These have been calculated on the basis that, if $w' = w(z) \cos \alpha y$, a streamfunction for the perturbation flow [which is in the (y, z) plane] is given by $\psi = -\alpha^{-1} w(z) \sin \alpha y$. Accordingly, the streamlines are given by

$$w(z) \sin \alpha y = \gamma, \tag{21}$$

where γ is a constant, $-1 \leqslant \gamma \leqslant 1$, if $w(z)$ has been normalized as above. For $R_H = 0$ the rolls are of square cross-section. In the centre of the layer, where the magnitude of z is small, the streamlines are approximately circles (a fact which can easily be predicted analytically). The tendency towards the development of boundary layers and multiple vortices as R_H increases is clear. In Fig. 2(c) the two vortices shown are contrarotating. The cross-section of each vortex is approximately square. In Fig. 2(d) the weak central vortex rotates in a sense opposite to that of the other two vortices. (Incidentally, for $R_H = 110$ an even mode, for which $w(z)$ has two peaks and a trough but is of constant sign, is a close competitor for the favoured mode. If it had been favoured then each roll would have contained two vortices inside a third, all co-rotating.)

Table 1. Critical values at the onset of instability

R_H	R_V	α	Symmetry
0	39.48	3.14	even
10	42.01	3.14	even
20	49.56	3.15	even
30	62.28	3.16	even
40	79.24	3.20	even
50	100.9	3.28	even
60	126.4	3.51	even
70	154.0	4.22	even
80	161.9	7.78	odd
90	143.5	7.73	odd
100	123.3	7.67	odd
110	101.4	7.61	odd
120	62.0	9.51	even
132.5	0	9.64	even

DISCUSSION

It was pointed out by Nield [1] that the effect of the horizontal temperature gradient on the instability of the longitudinal modes arises from $-\langle w\theta D\tilde{T}\rangle$, which can be interpreted as a rate of transfer of energy into the disturbance by interaction of the perturbation convective motion with the basic temperature gradient. Thus, we have a situation which contrasts with the instability of shear flows in a clear fluid, in which a mechanism involving a transfer of momentum is involved.

From equation (12) we have

$$D\tilde{T} = -R_V + \frac{1}{24} R_H^2 (1 - 12z^2). \tag{22}$$

The effect of increasing R_H is to distort the basic temperature profile away from the linear one. For small R_H the effect of increasing R_H is stabilizing because the negative temperature gradient is decreased in magnitude in the bulk of the fluid. For $R_H \geqslant 50$ one finds (using the data in Table 1) that the temperature gradient is positive in the centre of the layer (where z is small). As R_H increases the gradient in the centre becomes more and more positive, but that in regions nearer the walls becomes more and more negative. For large R_H the "dividing" levels at which $D\tilde{T} = 0$ are given by $z = \pm 0.29$ approximately. Thus, it is to be expected that R_V will eventually decrease as R_H increases, and that the bulk of the perturbation flow will be outside the vertically central portion of the layer.

When θ is eliminated between (17) and (18), one has

$$(D^2 - \alpha^2 + i\sigma - ikU)(D^2 - \alpha^2)w - ikR_H Dw + \alpha^2 (D\tilde{T})w = 0, \tag{23}$$

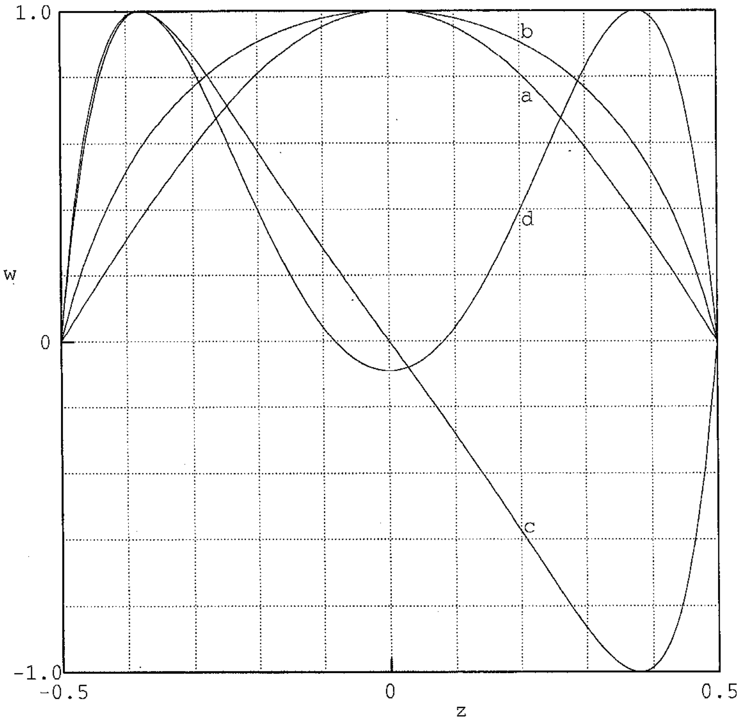

Fig. 1. Plots of the vertical velocity amplitude function $w(z)$, normalized so that the maximum magnitude is unity: (a) $R_H = 0$; (b) $R_H = 70$; (c) $R_H = 80$; (d) $R_H = 132.53$.

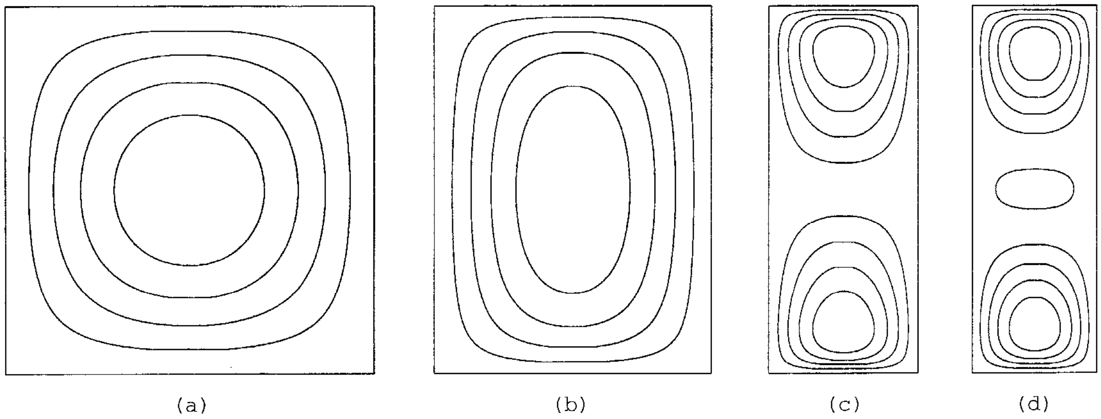

Fig. 2. Streamlines for the perturbation flow: (a) $R_H = 0$; (b) $R_H = 70$; (c) $R_H = 80$; (d) $R_H = 132.53$. For cases (a) and (b), streamlines have been drawn for $\gamma = 0.2$, 0.4, 0.6 and 0.8, where γ is as in equation (5). For case (c) the streamlines are drawn for $\gamma = \pm 0.2, \pm 0.4, \pm 0.6, \pm 0.8$. For case (d), the middle streamline corresponds to $\gamma = -0.5$, and the others (two branches for each value) correspond to $\gamma = 0.2, 0.4, 0.6, 0.8$.

and when $k = \sigma = 0$ this reduces to

$$(D^2-\alpha^2)^2 w+\alpha^2(D\tilde{T})w = 0. \qquad (24)$$

The "dividing" values of z will give transition points for the asymptotic solution for $w(z)$ as R_H becomes large, and rough analysis indicates that that solution will have multiple peaks and troughs with spacing of order $R_H^{-1/2}$ in the central region, between the transition points.

As far as the author is aware, there are no experimental observations available on the present topic.

Acknowledgement—The author is grateful to Prof. D. M. Ryan for suggesting the method employed to determine the zeroes of determinants.

REFERENCES

1. D. A. Nield, Convection in a porous medium with inclined temperature gradient, *Int. J. Heat Mass Transfer* **34,** 87–92 (1991).
2. D. A. Nield, Convection in a porous medium with inclined

temperature gradient and horizontal mass flow, *Proc. Ninth Int. Heat Transfer Conf.*, Vol. 5, pp. 153–158. Hemisphere, Washington, DC (1990).
3. D. A. Nield, D. M. Manole and J. L. Lage, Convection induced by inclined thermal and solutal gradients in a shallow horizontal layer of a porous medium, *J. Fluid Mech.* **257**, 559–574 (1993).
4. J. E. Weber, Convection in a porous medium with horizontal and vertical gradients, *Int. J. Heat Mass Transfer* **17**, 241–248 (1974).
5. A. E. Gill, A proof that convection in a porous vertical slab is stable, *J. Fluid Mech.* **35**, 545–547 (1969).
6. B. Straughan, A nonlinear analysis of convection in a porous vertical slab, *Geophys. Astrophys. Fluid Dyn.* **42**, 269–276 (1988).
7. D. A. S. Rees, The stability of Prandtl–Darcy convection in a vertical porous layer, *Int. J. Heat Mass Transfer* **31**, 1529–1534 (1988).
8. J. G. Georgiadis and I. Catton, Free convective motion in an infinite vertical porous slot: the non-Darcian regime, *Int. J. Heat Mass Transfer* **28**, 563–572 (1985).
9. P. G. Daniels, P. A. Blythe and P. G. Simpkins, Thermally driven shallow flow in porous media: the intermediate regime, *Proc. R. Soc. Lond.* **A406**, 263–285 (1986).

Pergamon

Int. J. Heat Mass Transfer. Vol. 37, No. 18, pp. 3025–3030, 1994

0017-9310/94 $7.00+0.00

Comparison of convective heat transfer to perimeter and center jets in a confined, impinging array of axisymmetric air jets

AARON M. HUBER and RAYMOND VISKANTA†

Heat Transfer Laboratory, School of Mechanical Engineering, Purdue University, West Lafayette, IN 47907-1288, U.S.A.

(*Received* 27 *September* 1993 *and in final form* 12 *February* 1994)

INTRODUCTION

Heat transfer is enhanced through jet impingement for many different applications, including the tempering and shaping of glass, the annealing of metal and plastic sheets, the cooling of gas turbine blades, and the drying of textiles, veneer, paper, and film materials. However, a disadvantage of impingement heating or cooling can be the nonuniformity of the heat flux distribution. For large arrays the majority of jets will be center jets, i.e. surrounded on all sides by adjacent jets. However, for small arrays, a significant fraction of the impingement surface is covered by perimeter or boundary jets which are not completely surrounded by adjacent jets. For improved understanding of the flow and heat transfer in small arrays, the similarities and differences between the center jet and perimeter jets in a 3 by 3 square array ($X_n/D = 6.0$) were studied. Only limited local heat transfer coefficient data have been reported in the literature [1], and no known study examined the differences between a center and perimeter jet in a small array. Hence, local Nusselt numbers were obtained for $Re_D = 10\,200$ and $17\,000$ at $H/D = 6.0$, 1.0, and 0.25 with open spent air exits similar to the conditions used by Huber and Viskanta [2]. Symmetry was assumed and the convective coefficients were measured only over the lower quadrant shown in Fig. 1. This was done to keep the data files manageable in size.

The heat transfer coefficients were measured using a heated 0.025 mm thick stainless steel foil impingement surface coated with liquid crystals. The temperature distribution along the surface was determined by measuring the reflected wavelength of light from the liquid crystals with the use of bandpass filters and an electronic digitizer. With this technique local Nusselt number distributions are obtained that show the uniformity of coverage along the impingement surface. The experimental method and conditions are discussed in detail by Huber and Viskanta [2] and Huber [1].

RESULTS AND DISCUSSION

Local Nusselt numbers

The local Nusselt numbers are presented by contour and three-dimensional plots for the measurement area shown in Fig. 1. While experimental data were obtained for two Reynolds numbers, 10 200 and 17 000, the largest differences

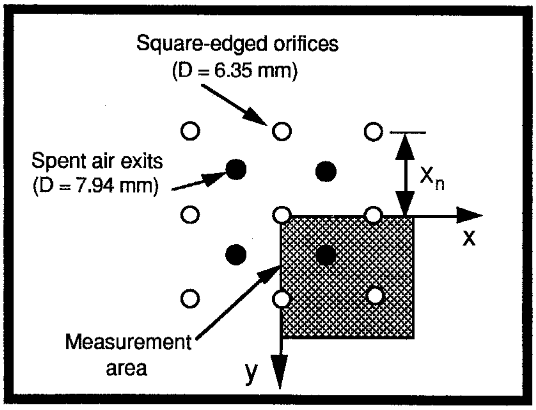

Fig. 1. Measurement area for perimeter jet experiments.

†Author to whom correspondence should be addressed.